

Anthocyanins/chitosan films doped by nano zinc oxide for active and intelligent packaging: comparison of anthocyanins source from purple tomato or black wolfberry

Yana Li (✉), Zenghui Li, Yuwen Wang, Liangbo Sun, Houchang Pei

School of Mechanical Engineering, Wuhan Polytechnic University, Wuhan 430023, China

© Higher Education Press 2023

Abstract The multifunctional films was prepared by blending chitosan and nano-ZnO with purple tomato anthocyanins or black wolfberry anthocyanins. The properties of films functioned by anthocyanins source and nano-ZnO content were studied. It was found purple tomato anthocyanins showed more significant color change against pH than black wolfberry anthocyanins. The nano-ZnO were widely dispersed in matrix and enhanced the compatibility of anthocyanins with chitosan. However, the anthocyanins source influenced the properties of the films more slightly than nano-ZnO addition. The tensile strength, antioxidant and antibacterial effects of the chitosan films dramatically increased after cooperated by nano-ZnO and anthocyanins, which also enhanced with increase of nano-ZnO content, whereas the elongation at break of the composite films decreased. Especially, the anthocyanin and nano-ZnO promoted the antibacterial activity of films synergistically. Composite films made from black wolfberry anthocyanins exhibited higher mechanical performance than those made from purple tomato anthocyanins but weaker antibacterial effects. The purple tomato anthocyanins/chitosan and nano-ZnO/purple tomato anthocyanins/chitosan films effectively reflected pork spoilage, changing their colors from dark green to brown, indicating the potential for applications in active and intelligent food packaging.

Keywords bio-based, multifunction, colorimetric indicator, active and intelligent packaging

1 Introduction

The design and development of biodegradable and multifunctional (e.g., antibacterial, antioxidant, pH-sensitive,

and ultra-violet shielding) packaging films based on natural polysaccharides (e.g., chitosan, pectin, starch, and cellulose) have attracted considerable interest [1]. In particular, chitosan has been developed as a food packaging material because of its excellent film-forming properties and biodegradability [2]. Some natural active substances extracted from agricultural products and food waste, such as polyphenols [3], essential oils [4], and plant extracts [5], are commonly combined with chitosan to enhance the antioxidant and antimicrobial activities of the films.

Anthocyanins are one of water-soluble, natural and nontoxic pH-sensitive pigments that are ubiquitous in nature with popular pharmacological antioxidant function [6]. Therefore, many researchers combined chitosan with anthocyanin to prepare active and intelligent packaging films [1]. The films based on anthocyanins from red cabbage, purple sweet potato, blueberry, black carrot, and other dark purple and black vegetables have been reported [7]. However, similar to the other biodegradable polymers, anthocyanins/chitosan films suffer from poor mechanical and barrier properties, which limit their use in packaging [8].

ZnO nanoparticles, which are approved by the Food and Drug Administration and generally recognized as safe [9], are widely used in packaging materials and food preservation because of their excellent chemical stability, antibacterial properties, and biocompatibility [10]. The incorporation of ZnO nanoparticles into polymer can significantly improve the mechanical and antibacterial properties of the matrices [11]. Also there have been many studies on ZnO nanoparticles-based smart indicator films recently. Yang et al. [12] prepared a two-layer colorimetric film composed of gelatin-nano ZnO and gellan gum-mulberry anthocyanin as the upper and lower films. The color stability of the biofilm was improved with the increase of nano-ZnO content, and the corruption of crucian carp was monitored. Sun et al. [13] used konjac glucomannan/chitosan with nano-ZnO and

mulberry anthocyanin extract to prepare a multifunctional biological nanocomposite film for food packaging. Nano-ZnO enhanced the antioxidant, antibacterial activities, and tensile strength of the composite film. Liu et al. [1] prepared a pH-sensitive antibacterial film by combining anthocyanins extracted from purple sweet potato or roselle into chitosan/polyvinyl alcohol/nano-ZnO matrix and conducted a comparative study. The results showed that the films exhibited high antibacterial activity and facilitated the monitoring of the degree of shrimp spoilage.

Though it was found the functional and physical properties of films dramatically depend on the sources of anthocyanins [8], no studies have been conducted specifically on the combination of chitosan and anthocyanins from different source with zinc oxide nanoparticles to form active films. Till now, there are also rare reports on purple tomatoes anthocyanins or black wolfberry anthocyanins used in intelligent packaging. As far as we know, one study found that chitosan films with the addition of purple tomato anthocyanins had significant color changes at different pH values and were able to change the properties of the films such as tensile strength and elongation at break, indicating the potential of such film as colorimetric indicators [9]. Recently, Kan et al. [14] compared the functionality of the films containing anthocyanins from different plant sources. They found the films with highly acylated anthocyanins were more suitable for monitoring food freshness. Some previous studies have shown purple tomato anthocyanins and black goji berry anthocyanins are highly acylated anthocyanins [15]. Meanwhile, the films containing purple tomato anthocyanins and black goji berry anthocyanins are effective in monitoring food freshness [9,16,17].

Therefore, in the present study, anthocyanins extracted from purple tomatoes (*Solanum lycopersicum*) and black wolfberry (*Lycium ruthenicum*) were used to prepare nano-ZnO/purple tomato anthocyanin/chitosan (ZP/PTA/CS) and nano-ZnO/black wolfberry anthocyanin/chitosan (ZP/BWA/CS) composite films for a comparative study. The performance of ZP/PTA/CS and ZP/BWA/CS films was evaluated on the basis of pH sensitivity, morphology, and mechanical property. In addition, possible interactions between fractions in the composite films were explored, as well as the relationship between the antioxidant and antimicrobial activity of the composite films and the ZnO nanoparticle content and anthocyanin source. A better performing composite film was also selected for monitoring the freshness and spoilage of pork.

2 Experimental

2.1 Materials

CS was purchased from Sinopharm Chemical Reagent

Co., Ltd. (Shanghai) with 91% deacetylation and 50 kDa of M_w . PTA and BWA were extracted from purple tomato and black wolfberry, respectively, according to a previously described method [9]. ZP with an average particle size of 50 nm was purchased from Nanjing Haitai Zinc Products Factory in China. Acetic acid, hydrochloric acid, and sodium hydroxide were purchased from Guangdong Guang Xiao Reagent Technology Co. *Escherichia coli* was provided by College of Food Science and Technology of Wuhan Polytechnic University. The pork (pork loin) was bought from Zhongbai supermarket in Wuhan. All other reagent-grade chemicals and solvents were purchased from Shanghai Maclean Biochemical Technology Co. (Shanghai, China).

2.2 Preparation of nano-ZnO/anthocyanins/chitosan composite films

The films were prepared with the solution casting method according to references of [7,8] and the content of CS, ZP, and anthocyanins in them was shown in Table 1. Firstly, 2 g of CS was dissolved in 100 mL of 1.0% (v/v) acetic acid in aqueous solution and stirred at room temperature for 4 h at $800 \text{ r} \cdot \text{min}^{-1}$. Then, 5% weight (based on w/w of CS) of PTA or BWA was added to respective CS solutions and stirred at $800 \text{ r} \cdot \text{min}^{-1}$ for 4 h. Afterwards, 0.01 g or 0.02 g of ZP was added and stirred again for 4 h prior to sonication for 30 min. The obtained nano-ZnO/anthocyanins/chitosan solutions were poured in a Petri dish with a diameter of 15 cm and dried at 40°C and 50% relative humidity for 24 h. The resulting ZP/PTA/CS and ZP/BWA/CS composite films were stored in a desiccator at 25°C and 50% relative humidity before characterization.

2.3 pH-sensitivity of anthocyanins

Hydrochloric acid, sodium hydroxide and purified water were used in preparing buffers with pH of 2–12, and 5 mL of PTA or BWA ($1000 \text{ mg} \cdot \text{L}^{-1}$) solutions were mixed with 10 mL of the buffers [18]. All anthocyanin solutions were photographed, and the spectra of anthocyanin solutions with pH of 2–12 were measured at 200–700 nm with ultra-violet–visible spectroscopy (UV–vis) (GNilent CARY 100, Varian Corporation, USA) [8].

Table 1 Formulation of composite films with different mass fractions

Sample	CS/g	Anthocyanins/g	ZnO nanoparticles/g
CS	2	0	0
PTA/CS	2	0.1	0
0.5%-ZP/PTA/CS	2	0.1	0.01
1%-ZP/PTA/CS	2	0.1	0.02
BWA/CS	2	0.1	0
0.5%-ZP/BWA/CS	2	0.1	0.01
1%-ZP/BWA/CS	2	0.1	0.02

2.4 Characterization of nano-ZnO/anthocyanins/chitosan composite films

2.4.1 Color, thickness and UV-vis spectra of composite films

The luminance (L), red-green values (a), and yellow-blue values (b) of the films were determined using a colorimeter (Konica Minolta, Model CR-20, Japan) with a standard white plate ($L^* = 92.9$, $a^* = 0.32$, and $b^* = 0.33$) as a background [19]. The total color difference (ΔE) and whiteness index (WI) of the films were calculated as follows [18]:

$$\Delta E = \sqrt{(L^* - L)^2 + (a^* - a)^2 + (b^* - b)^2}, \quad (1)$$

$$WI = 100 - \sqrt{(100 - L)^2 + a^2 + b^2}, \quad (2)$$

where L , a , and b are the color parameters of the colorimetric films.

The thickness of the laminated film was measured at five random locations on the film with a thickness tester (SM-114, Shanghai Liuling Instrument Factory, China) [20]. The average thickness value was calculated for each sample.

The film samples (2 cm × 2 cm) were attached to a UV cuvette placed in a UV-vis spectrophotometer (756PC, Shanghai Haoyu Hengping Scientific Instruments Co., Ltd., Shanghai, China) for the determination of UV-vis transmittance at wavelengths from 200 nm to 700 nm [8].

2.4.2 Morphology and Fourier transform infrared (FTIR) spectroscopy

The surface and cross-sectional morphology of the films fractured in liquid nitrogen were observed through scanning electron microscopy (SEM, SU-8010, HITACHI Co., Ltd., Japan) [21].

The FTIR spectra of the films were measured by using an FTIR spectrophotometer (Tensor 27, Bruker Optics, Germany) from 4000 to 500 cm^{-1} at a resolution of 4 cm^{-1} [22].

2.4.3 Color response, moisture content, mechanical properties, and contact angle

The pH sensitivity of the film samples was determined according to the method described by Qin et al. [23]. Each film was pictured after being immersed in buffer solutions (pH 2–12) for 5 min.

The composite films (0.5 g) were dried at 105 °C to constant weight, and moisture content was calculated according to the following formula [20]:

$$\text{Moisture content (\%)} = \frac{w_1 - w_2}{w_1}, \quad (3)$$

where w_1 and w_2 are the initial and final weights of the film, respectively.

The mechanical properties of the films were measured with a tensile machine (WDW-10C, Shanghai, China) equipped with a 500 N pressure measuring element [2]. The evaluation was performed at 25 °C at 60% relative humidity with the ASTM D882-18 method (ASTM, 2018). Film samples were cut into small strips (100 mm × 15 mm) and evaluated for tensile strength (TS) and elongation at break (EB).

The fabricated composite films were cut into 2 cm × 5 cm films, and each specimen was measured in three parallel experiments. The contact angle values were obtained when the contact time of water and film were 10 s by using a contact angle tester (JCY, Shanghai Fangrui Instruments Co., Ltd.) [2]. The average contact angle of six different measurements was taken as the final result.

2.4.4 Antioxidant properties and antibacterial property

Antioxidant activity was evaluated according to its ability to scavenge DPPH radicals. Briefly, 50 mg of the film sample was immersed in 50 mL of 95% ethanol and gently stirred at 50 $\text{r} \cdot \text{min}^{-1}$ for 24 h. 0.1 mL of the sample solution was mixed with 4 mL of 0.1 $\text{mmol} \cdot \text{L}^{-1}$ DPPH dissolved in methanol. The reaction was carried out in the dark at room temperature (25 ± 2 °C) for 30 min [24]. The absorbance of the reaction mixture at 517 nm was then characterized. Each sample had three replicates. The DPPH scavenging activity was calculated as follows [25]:

$$\text{DPPH radical scavenging activity (\%)} = \frac{A_0 - A_1}{A_0}, \quad (4)$$

where A_0 is the absorbance of the control solution and A_1 is the absorbance of the test film reaction solution.

The bacterial inhibitory activities of the films was determined with the filter paper method and a disc inhibition assay against *Escherichia coli* [26]. The filter paper (6 mm in diameter) was soaked in the film-forming solutions at room temperature for 24 h. After removal, the surface was blotted dry with filter paper and dried at 60 °C. The microbial strain was activated with 10 mL of nutrient broth at 37 °C and shaken in a water bath shaker for 3 h. Then, 100 μL of the prepared bacterial suspension was evenly coated on the agar medium with an applicator, and the filter paper was taped on solid culture medium surface. Lastly, the petri dishes were incubated at 37 °C for 24 h, the zone of inhibition was measured with Vernier calipers, and the antibacterial rate was calculated using Eq. (5) [11].

$$\text{Antibacterial rate (\%)} = \frac{d_1 - d_2}{d_2}, \quad (5)$$

where d_2 is the diameter of the black and d_1 is the diameter of a sample.

2.5 Application in intelligent packaging

The ZP/PTA/CS, 0.5%-ZP/PTA/CS, and 1%-ZP/PTA/CS films were used in monitoring pork spoilage during storage, and the CS film was used as the control. A film sample (2 cm × 2 cm) was placed beside a pork sample (30 g) on the bottom of a disposable bacterial Petri dish with a diameter of 9 cm, and then the Petri dishes were stored at 5 °C for 96 h. Color changes in the composite films were photographed at five time points (0, 24, 48, 72, and 96 h). Approximately 10 g of pork was homogenized in 90 mL of distilled water. Each sample had three replicates, and the pH of the pork samples was measured using a digital pH meter (PhS-3E, INESA Scientific Instruments Co., Ltd., China) three times at 0, 24, 48, 72, and 96 h [18]. Simultaneously, the total volatile essential nitrogen (TVB-N) of the pork was determined according to Li et al. [9] with a semi-micro Kjeldahl distillation instrument.

2.6 Statistical analysis

Multiple samples were tested, and the means and standard deviations (SD) were calculated. Analysis of variance was performed using SPSS 22.0 for the evaluation of differences between single factors and levels. Duncan's multiple interval test of comparison was used in determining which groups are significantly different from others ($p \leq 0.05$).

3 Results and discussion

3.1 Original films

The original appearance and UV-vis spectra of films are shown in Fig. 1. The chitosan film changed from transparent to green color when combined with anthocyanins. Interestingly, the colors of PTA/CS films deepened with

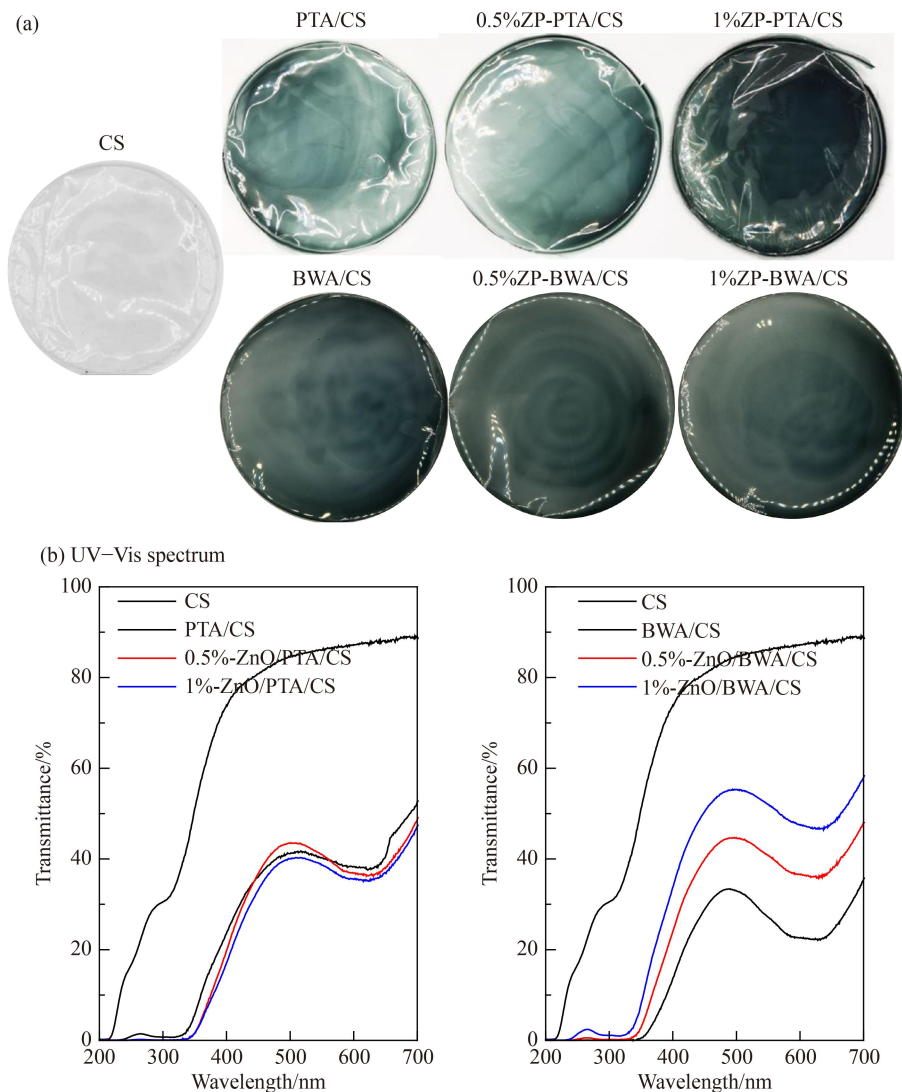


Fig. 1 (a) Digital photos and (b) UV-vis spectrum of films.

increasing ZP content, but the BWA/CS films showed nearly no change. In a range of 500–850 nm, the transmittance of the film was significantly reduced after the addition of PTA or BWA relative to that of the CS film probably because anthocyanin has the maximum absorption wavelength in this interval [8,12]. The color parameters of the composite films are shown in Table 2. After the addition of PTA or BWA, the L , a , and WI of the CS films decreased significantly ($P < 0.05$), whereas the b and ΔE values increased ($P < 0.05$). These results indicated that the overall surface brightness of the composite film decreased and the total color difference increased, resulting in a significant decrease in the light transmission of the composite films [27]. The color parameters of the composite films influenced by ZP were irregular.

3.2 pH sensitivity

3.2.1 Anthocyanins

Figure 2 shows the color change and UV-vis spectra of the PTA and BWA solutions under different pH conditions. In PTA, at pH of 2–6, the solution gradually changed from purplish red to colorless because it contained yellow salt cations [28]. At pH of 7–9, colorless chalcones and blue quinone-type bases [9] were present in the solution, and the solution gradually

changed from colorless to blue-green. At pH of 9–12, phenol salts [25,29] were generated, and the solution gradually changed from light yellow to orange-yellow. As for BWA, the solution gradually changed from pink to colorless at pH of 2–5. At pH of 6–9, the solution gradually changed from colorless to light blue. When pH increased to 10–12, BWA was gradually degraded to yellow-green. Figure 2 shows that the color response of PTA was more obvious than that of BWA, indicating the higher sensitivity of PTA to pH changes. The UV-vis spectra of PTA and BWA showed that similar characteristic peaks appeared under acidic conditions and no obvious characteristic peaks appeared in neutral and alkaline environments possibly because of the structural changes in anthocyanins at different pH [8]. These results suggested that PTA and BWA have good sensitivity to pH changes.

3.2.2 Nano-ZnO/anthocyanins/chitosan films

The color response of the composite films in Fig. 3 at different pH levels shows that the composite films reacted more obviously as a light red color at pH 2 after the addition of PTA or BWA, and that there was no particular change in color after the addition of ZnO nanoparticles. As shown in Fig. 3, the CS films were not sensitive to changes in pH, but the addition of PTA or BWA gave the composite films some pH sensitivity. In addition, the

Table 2 Color parameters of films

Films	L	a	b	ΔE	WI
CS	89.88 ± 0.15^a	2.58 ± 0.16^a	-2.72 ± 4.07^f	5.46 ± 0.84^f	88.72 ± 1.80^a
PTA/CS	43.86 ± 4.06^e	-6.34 ± 0.44^d	3.32 ± 0.28^b	49.56 ± 3.94^c	43.40 ± 4.05^{de}
0.5%-ZP/PTA/CS	46.28 ± 1.49^c	-7.02 ± 0.48^e	1.10 ± 0.34^e	45.07 ± 1.42^d	47.79 ± 1.46^c
1%-ZP/PTA/CS	37.86 ± 1.76^f	-6.16 ± 0.21^{cd}	2.70 ± 0.65^c	55.20 ± 1.65^a	37.49 ± 1.72^f
BWA/CS	51.52 ± 1.8^b	-6.34 ± 0.26^c	1.52 ± 0.35^d	41.88 ± 1.84^e	51.08 ± 1.84^b
0.5%-ZP/BWA/CS	42.60 ± 1.48^e	-5.34 ± 0.17^b	3.24 ± 0.19^a	51.47 ± 1.35^b	41.89 ± 1.43^e
1%-ZP/BWA/CS	45.3 ± 9.87^d	-6.6 ± 0.07^d	3.1 ± 0.25^b	48.18 ± 0.85^c	44.8 ± 0.87^d

Data are presented as mean \pm SD ($n = 3$). Data with different lower case superscript letters in the same column indicate that they are statistically different ($P < 0.05$).

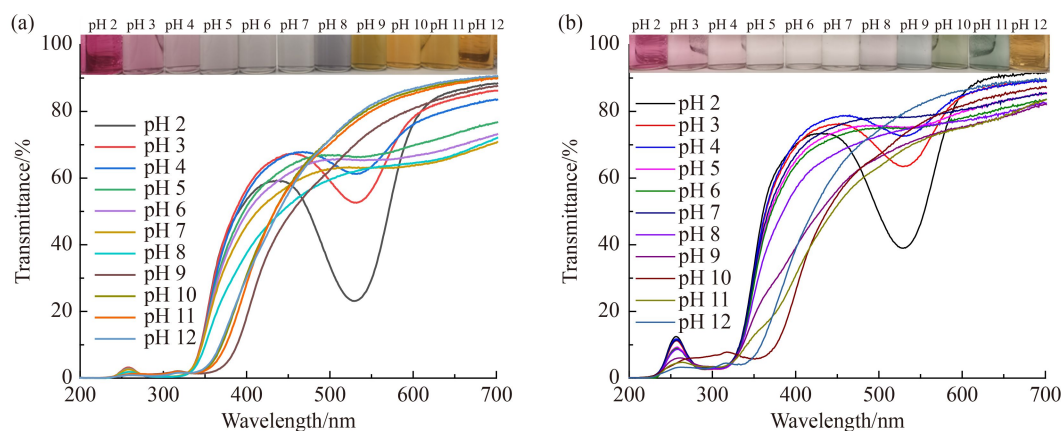


Fig. 2 pH-sensitivity of (a) PTA and (b) BWA.

color of the composite film did not change particularly significantly after the addition of ZnO nanoparticles, but the composite film did not show as pronounced a pH response as the pure anthocyanins. This may be due to the fact that the amount of anthocyanin added to the composite film was low, so it resulted in a less pronounced color response in the composite film.

3.3 Morphology

The SEM images of films are shown in Fig. 4. It was found the CS film had an even surface (Figs. 4(A–G)), then it became rough and showed a pore-like structure after the addition of PTA or BWA possibly because of the agglomeration of anthocyanins. However, the surfaces of the PTA/CS and BWA/CS films became gradually uniform as ZP content increased, suggesting that ZP increased the compatibility between anthocyanins and CS matrices. Especially, the BWA/CS film showed more

significantly change in surface morphology than the PTA/CS film, and thus the surfaces of the 0.5%-BWA/CS and 1%-BWA/CS films became completely flat.

Similarly, the cross-section of the CS film was smooth and homogeneous, as shown in Fig. 4(a). After the addition of PTA or BWA, the cross-section of the composite film was uneven with concave and convex areas, as shown in Figs. 4(b) and 4(e), and the smoothness and uniformity of the cross-sections of the composite films increased with the amount of ZnO nanoparticles, which indicates the ZP are well dispersed in the PTA/CS and BWA/CS films [30]. Furthermore, the cross-section of the BWA/CS film was smoother than that of the PTA/CS film, suggesting that BWA is more compatible with CS than PTA.

3.4 FTIR

Figure 5 exhibited the FTIR spectra of CS, PTA/CS, 1%-

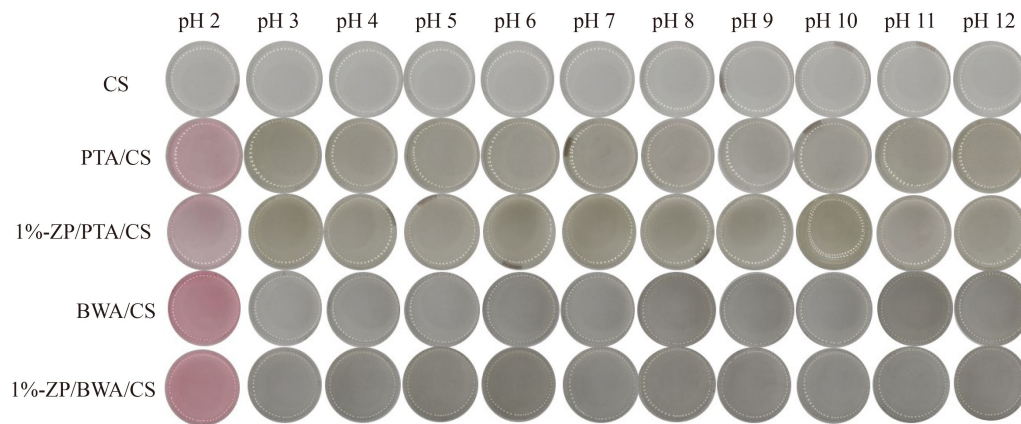


Fig. 3 Color of CS, PTA/CS, 1%-ZP/PTA/CS, BWA/CS and 1%-ZP/BWA/CS films in pH solutions.

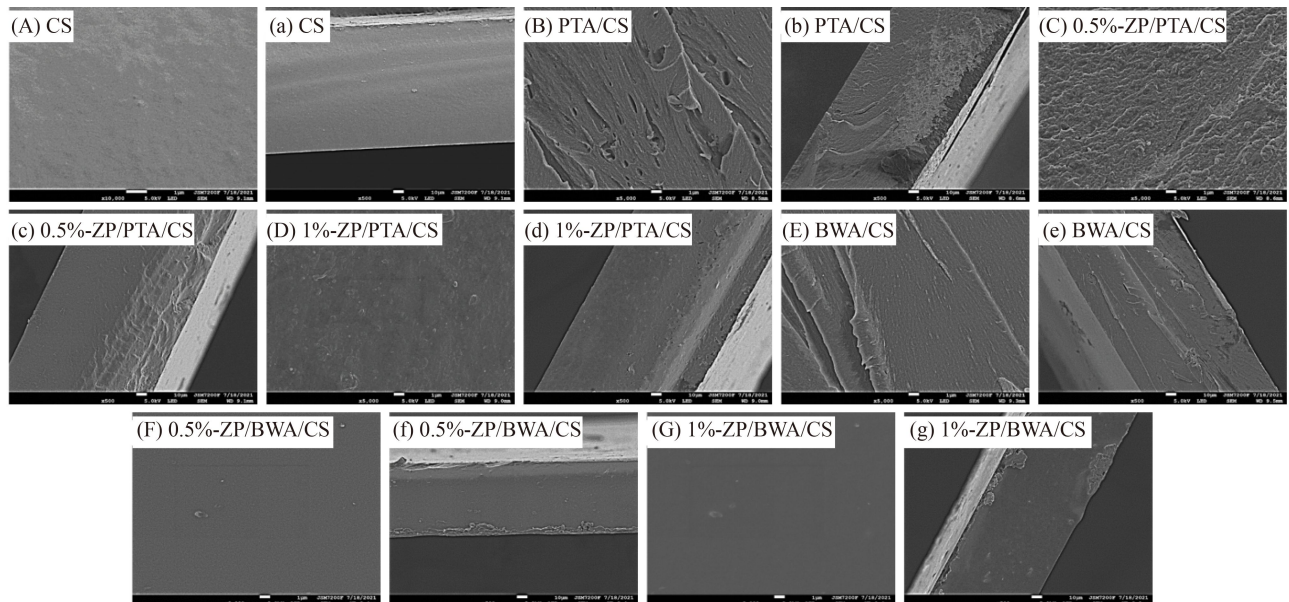


Fig. 4 SEM images of (A–G) films with surface and (a–g) cross section.

ZP/PTA/CS, BWA/CS and 1%-ZP/BWA/CS. The FTIR spectrogram of CS in Fig. 5 shows a broad band at 3530 cm^{-1} , which can be indexed to the stretching vibrations of pendant groups of -NH_2 and -OH in CS [31]. The band at 2870 cm^{-1} corresponds to the asymmetric stretching vibrations of $\text{-CH}_2\text{-}$ group in CS chain. The stretching vibration of C=O and C-N groups in CS is responsible for the bands at 1562 and 1408 cm^{-1} . Also the band obtained at 1020 cm^{-1} is caused by the stretching vibrations of the -C-O-C- linkage of CS [32].

As can be seen from the spectrograms of PTA/CS and BWA/CS in Fig. 5, the incorporation of PTA or BWA into the CS film results in a slight change in the position of the stretch band. The most significant change was a decrease in the intensity of the band at 3530 cm^{-1} , probably due to the interaction of the polyphenols in anthocyanins with the hydroxyl groups of chitosan [33]. In addition, the intensity reduction at 1562 cm^{-1} , is associated to the interaction between C=O of glycoside groups and C=C stretching vibration of the aromatic ring from anthocyanins with the N-H stretching vibration of amides from chitosan [33,34]. Therefore, the FTIR results showed in anthocyanins/chitosan composites, there are interactions between anthocyanins and chitosan. Furthermore, it can be seen that the PTA/CS film has a more pronounced wave variation than the BWA/CS film, which may be due to the PTA is more compatible with chitosan than BWA.

In addition, compared with the PTA/CS and BWA/CS films, a clear shift of the spectral band positions toward the lower and higher wave number regions is clearly seen for 1%-ZP/PTA/CS and 1%-ZP/BWA/CS films, which suggests a stronger interaction among chitosan, anthocyanins and ZnO nanoparticles. This is consistent with the results of Rahman et al. [32].

3.5 Thickness, moisture content, mechanical properties, and contact angle

The thickness, moisture content, TS , and EB of the indicator films are shown in Table 3. The thickness of the films significantly increased after the addition of PTA or BWA ($P < 0.05$) possibly because the fusion of CS and anthocyanins resulted in cohesion between them [35], which increased the density of the composite films. As the content of ZP increased, the thickness of the composite films gradually increased. The possible causes were the strong mobility and easy agglomeration of ZP and subsequent enhanced internal bonding between composite film fractions [1].

Table 3 shows that the CS film had the lowest moisture content, and the moisture content of the composite films increased significantly after the addition of PTA ($P < 0.05$) possibly because of the large amount of hydrophilic phenolic hydroxyl groups in anthocyanin. The moisture content of PTA/CS composite films increased gradually

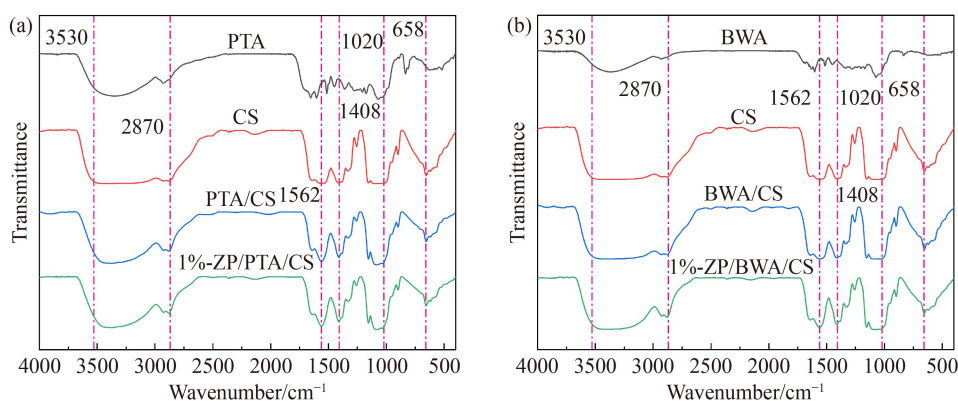


Fig. 5 FTIR spectra of films.

Table 3 Thickness, moisture content, mechanical properties and contact angle of films

Films	Thickness/ μm	Moisture content/%	TS/MPa	$EB/\%$	Contact angle/ $^\circ$
CS	$41 \pm 1^{\text{de}}$	$13.98 \pm 0.58^{\text{c}}$	$77.74 \pm 1.50^{\text{d}}$	$12.77 \pm 1.32^{\text{a}}$	$75.8 \pm 1.6^{\text{c}}$
PTA/CS	$45 \pm 6^{\text{e}}$	$16.54 \pm 0.26^{\text{b}}$	$80.83 \pm 5.58^{\text{cd}}$	$4.66 \pm 0.90^{\text{bc}}$	$75.5 \pm 0.6^{\text{c}}$
0.5%-ZP/PTA/CS	$51 \pm 4^{\text{ab}}$	$17.13 \pm 0.65^{\text{ab}}$	$82.81 \pm 2.79^{\text{bc}}$	$4.24 \pm 0.55^{\text{bc}}$	$81.0 \pm 3.4^{\text{b}}$
1%-ZP/PTA/CS	$58 \pm 7^{\text{a}}$	$17.86 \pm 0.18^{\text{a}}$	$83.37 \pm 3.58^{\text{bc}}$	$3.71 \pm 0.43^{\text{c}}$	$85.6 \pm 1.1^{\text{a}}$
BWA/CS	$45 \pm 4^{\text{bc}}$	$14.62 \pm 0.39^{\text{c}}$	$85.67 \pm 2.62^{\text{bc}}$	$4.90 \pm 0.79^{\text{b}}$	$75.4 \pm 0.6^{\text{c}}$
0.5%-ZP/BWA/CS	$48 \pm 4^{\text{c}}$	$13.85 \pm 0.26^{\text{c}}$	$87.01 \pm 2.51^{\text{b}}$	$4.51 \pm 0.54^{\text{bc}}$	$80.4 \pm 0.3^{\text{b}}$
1%-ZP/BWA/CS	$52 \pm 3^{\text{cd}}$	$14.24 \pm 0.57^{\text{c}}$	$90.60 \pm 1.99^{\text{a}}$	$4.70 \pm 1.23^{\text{bc}}$	$82.0 \pm 0.2^{\text{b}}$

Values are given as mean \pm SD ($n = 6$ for film thickness, $n = 3$ for moisture content and contact angle, and $n = 6$ for TS and EB). Different letters in the same column indicate significantly different ($P < 0.05$).

after the addition of ZP possibly because of hydrogen bonds of chitosan and PTA with the oxygen of ZP, which subsequently formed hydrophilic hydroxyl groups [1]. Rahman et al. [32] obtained the same results and they thought that the introduction of ZnO particles in the film led to the formation of cavities, paving the way for the adsorption of more water molecules and increasing the water content of the film. While, the moisture content of the BWA/CS composite films did not change significantly ($P > 0.05$) as a function of ZP, indicating that PTA has better hydrophilic properties than BWA.

As shown in Table 3, the TS increased after the addition of PTA or BWA. The probable reason was the generation of hydrogen bonds between molecules, which enhanced intermolecular interactions. The addition of BWA significantly enhanced the TS of the composite film ($P < 0.05$). As ZP concentration increased, the TS of the composite film showed an increasing trend possibly because of the high dispersion of ZP [1], which enhanced the bonding between the molecules of the composite film and that was confirmed by the results of FTIR. However, the EB decreased by 63.5% and 61.6% after the addition of PTA and BWA, respectively, because of the rigidity of anthocyanins, which limited the movement between polymer molecules. Moreover, the EB of the films was reduced by the doped ZP. Li et al. [36] found that the incorporation of ZnO nanoparticles improved the mechanical properties of chitosan films. It has been shown that the interfacial bonding between chitosan and nanoparticles leads to an effective transfer of stress to the nanoparticles, thus improving the mechanical properties of the composite film [37].

The water contact angle of the film surface is shown in Table 3. The data showed that the contact angle of the CS film had no significant change after the addition of PTA or BWA ($P > 0.05$). However, after blending with ZP, the contact angles of the films significantly improved ($P < 0.05$), indicating that the hydrophobicity of the composite films was dramatically enhanced [38] because of the reduction in the number of intermolecular gaps by nanoparticles [30,39]. The improved hydrophobicity rendered the film suitable for packaging materials.

3.6 Antioxidant property

A DPPH radical scavenging test was used in evaluating the antioxidant activities of the films. The results are shown in Fig. 6. The antioxidant performance of the CS film was relatively low, but the scavenging rate of the DPPH radicals of CS increased to 50.86% or 52.58% after the addition of PTA or BWA, respectively. This finding showed that PTA and BWA have high antioxidant activities and BWA has better antioxidant ability than PTA. Anthocyanins contain a large number of phenolic hydroxyl structures that can provide hydrogen atoms for scavenging free radicals [25,40]. Therefore, the addition

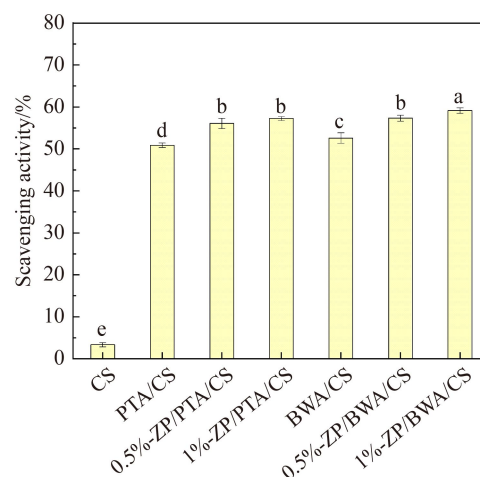


Fig. 6 DPPH radical scavenging activity of films.

of PTA or BWA can improve the antioxidant properties of CS films. The antioxidant properties of the ZP/PTA/CS and ZP/BWA/CS films increased with ZP concentration because of the high antioxidant properties of nano-ZnO [40].

3.7 Antibacterial property

Antibacterial ability was determined according to the size of inhibitory zone against *Escherichia coli*. As shown in Fig. 7, the CS film had a certain bacterial inhibition rate due to the antimicrobial properties of chitosan. These properties can be attributed to the presence of a large number of amino groups [41,42]. After the addition of PTA or BWA to the chitosan matrix, the bacterial inhibition rate of the composite films increased, and the PTA/CS films showed a more significant increase ($P < 0.05$), demonstrating the better bacterial inhibition effect of PTA. Moreover, anthocyanins disrupt microbial cell films and bacterial metabolism and promote bacterial content release and bacterial decomposition [43]. The antibacterial activities of the composite films gradually increased after the addition of ZP and was further enhanced by increase in ZP content because of the antibacterial of ZP [40]. ZnO nanoparticles can make the surrounding hydroxyl electron loss into free radicals, as a strong oxidant to degrade organic matter and kill bacteria and viruses [13]. The above results indicate that anthocyanin and nano-ZnO have a synergistic effect on the improvement of antibacterial activity for the composite film.

3.8 Application to intelligent packaging

The products of microorganisms affect the freshness of pork, which contains large amounts of protein and fat, and cause the breakdown of proteins into peptone, peptides, and amino acids, which are further broken down

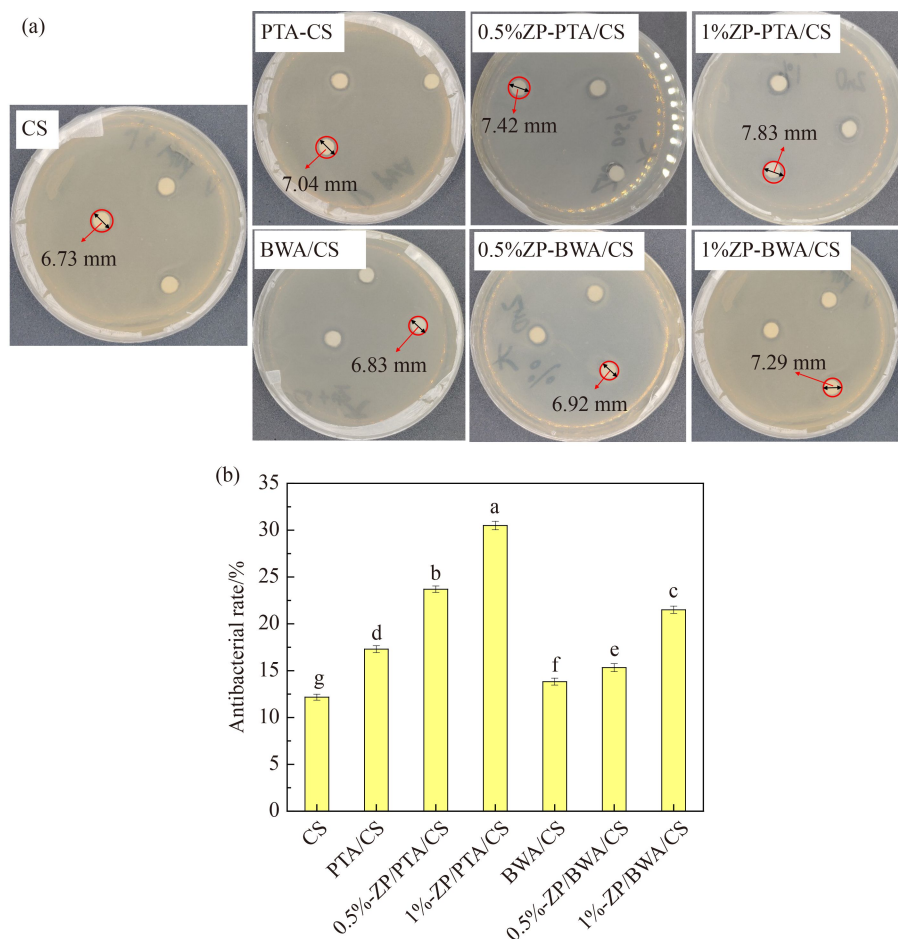


Fig. 7 (a) Zone of inhibition and (b) antibacterial rate of films against *Escherichia coli*.

into ammonia, hydrogen sulfide, phenols, amines, and carbon dioxide. These products lead to spoilage and pH changes in pork [44]. Therefore, the pH value of pork was used as the parameter of pork freshness. Table 4 indicates the color response of the CS and ZP/PTA/CS films used to detect the pork freshness at different storage times and corresponding pH and TVB-N values.

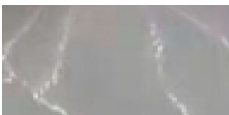
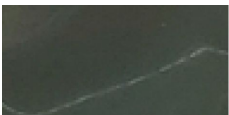
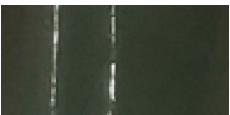
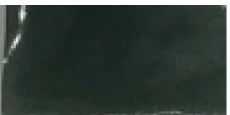
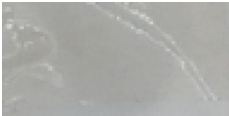
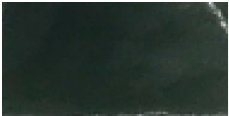
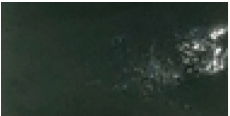

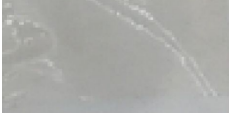
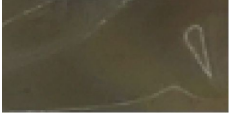
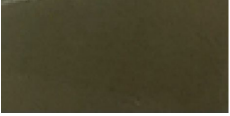
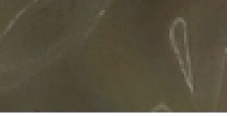
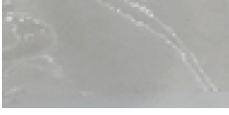
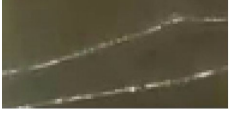
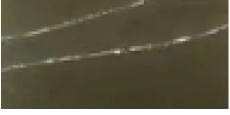
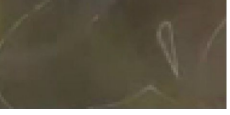

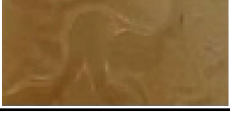
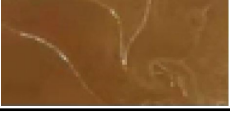
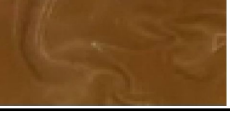
As shown in Table 4, the pH and TVB-N of pork increased with storage time, indicating the gradual deterioration of pork. Before the addition of PTA, the composite film was dark green during whole storage. However, its color changed to dark gray at 24 h after the addition of PTA, while the corresponding TVB-N of pork was 10.67 mg/100 g. The PTA-based films gradually changed to gray-brown at 48 h and 72 h with 12.15 mg/100 g and 14.36 mg/100 g of TVB-N, respectively, then changed to brown at 96 h (TVB-N = 18.65 mg/100 g). For pork, it was fresh with the TVB-N content of 8.02 mg/100 g at 0 h according to Chinese standard (GB2707-2016), which was specified that the TVB-N content of fresh pork should be less than 15 mg/100 g. Thus, the pork sample was completely spoiled at 96 h. That suggests the ZP/PTA/CS films can detect the deterioration of pork and can be applied to intelligent packaging. Furthermore, it is

interesting that ZP addition improved the color-sensitive of PTA for the composite films. However, the color response of the films against pH in food packaging was not consistent with that in pH solutions, which was also found in our other studies [9], and the mechanisms will to be studied in the future.

4 Conclusions

In this study, functional nano-ZnO/anthocyanins/chitosan films were successfully prepared by adding PTA or BWA and nanoparticles to CS matrices. Color change in PTA was more obvious than that of BWA under varying pH. The FTIR data revealed that PTA was more integrated with chitosan than BWA and that ZnO nanoparticles were able to interact chemically with the composite film. The addition of PTA or BWA changed the internal structure of the CS matrix, and ZP enhanced the compatibility of PTA or BWA with chitosan, improving Mechanical properties of the composite films. Moreover, the nano-ZnO/anthocyanins/chitosan films showed excellent antioxidant and antibacterial properties in contrast to the CS film, and the antioxidant and antibacterial properties

Table 4 Color variation of films against pH and TVB-N of pork during storage time

Time/h	pH value of pork	TVB-N content (mg per 100 g)	Color variation of films			
			CS	PTA/CS	0.5%-ZP/PTA/CS	1%-ZP/PTA/CS
0	5.49 ± 0.02	8.02 ± 0.11				
24	5.57 ± 0.015	10.67 ± 0.32				
48	5.68 ± 0.01	12.15 ± 0.08				
72	6.07 ± 0.01	14.36 ± 0.54				
96	6.42 ± 0.01	18.65 ± 0.57				

increased with ZP content. The anthocyanin and zinc oxide have a well synergistic improvement on the antibacterial activity of films. The PTA film showed better color response to pH and higher antibacterial properties against *Escherichia coli* than the BWA film. No significant difference in physiochemical performance influenced by anthocyanin source was found. Finally, the ZP/PTA/CS films were effective in monitoring the freshness of pork. These findings indicated that the nano-ZnO/anthocyanins/chitosan composite films have potential uses in active and intelligent packaging.

Acknowledgements This research received funding from the Research and Innovation Initiatives of WHPU (Grant No. 2023Y29).

References

- Liu J Y, Huang J Y, Ying Y B, Hu L P, Hu Y Q. pH-sensitive and antibacterial films developed by incorporating anthocyanins extracted from purple potato or roselle into chitosan/polyvinyl alcohol/nano-ZnO matrix: comparative study. *International Journal of Biological Macromolecules*, 2021, 178: 104–112
- Li Y N, Ren J Z, Wang B H, Lu W Q, Wang H X, Hou W F. Development of biobased multilayer films with improved compatibility between polylactic acid-chitosan as a function of transition coating of SiO_x. *International Journal of Biological Macromolecules*, 2020, 165: 1258–1263
- Nazareth M S, Shreelakshmi S V, Rao P J, Shetty N P. Micro and nanoemulsions of *Carissa spinarum* fruit polyphenols, enhances anthocyanin stability and anti-quorum sensing activity: comparison of degradation kinetics. *Food Chemistry*, 2021, 359: 129876
- Tao R, Sedman J, Ismail A. Antimicrobial activity of various essential oils and their application in active packaging of frozen vegetable products. *Food Chemistry*, 2021, 360: 129956
- Bigi F, Haghighi H, Siesler H W, Licciardello F, Pulvirenti A. Characterization of chitosan-hydroxypropyl methylcellulose blend films enriched with nettle or sage leaf extract for active food packaging applications. *Food Hydrocolloids*, 2021, 120: 106979
- Wu C H, Li Y L, Sun J S, Lu Y Z, Tong C L, Wang L, Yan Z M, Pang J. Novel konjac glucomannan films with oxidized chitin nanocrystals immobilized red cabbage anthocyanins for intelligent food packaging. *Food Hydrocolloids*, 2020, 98: 105245
- Qin Y, Liu Y P, Yuan L M, Yong H M, Liu J. Preparation and characterization of antioxidant, antimicrobial and pH-sensitive films based on chitosan, silver nanoparticles and purple corn extract. *Food Hydrocolloids*, 2019, 96: 102–111
- Yan J T, Cui R, Tang Z Y, Wang Y R, Wang H, Qin Y Y, Yuan M W, Yuan M L. Development of pH-sensitive films based on gelatin/chitosan/nanocellulose and anthocyanins from hawthorn (*Crataegus scabrifolia*) fruit. *Journal of Food Measurement and Characterization*, 2021, 15(5): 3901–3911
- Li Y N, Wu K X, Wang B H, Li X Z. Colorimetric indicator based on purple tomato anthocyanins and chitosan for application in intelligent packaging. *International Journal of Biological Macromolecules*, 2021, 174: 370–376
- Jamnonngkan T, Yosta A, Thanesthakul B, Sugimoto M, Hara T, Takatsuka Y, Mongkholrattanasit R. Effect of ZnO nanoparticles on the physical properties of PLA/PBS biocomposite films. *Materials Science Forum*, 2021, 1033: 143–150

11. Li S C, Li Y N. Mechanical and antibacterial properties of modified nano-ZnO/high-density polyethylene composite films with a low doped content of nano-ZnO. *Journal of Applied Polymer Science*, 2010, 116(5): 2965–2969
12. Yang Z K, Zhai X D, Zou X B, Shi J Y, Huang X W, Li Z H, Gong Y Y, Holmes M, Povey M, Xiao J B. Bilayer pH-sensitive colorimetric films with light-blocking ability and electrochemical writing property: application in monitoring crucian spoilage in smart packaging. *Food Chemistry*, 2021, 336: 127634
13. Sun J S, Jiang H X, Wu H B, Tong C L, Pang J, Wu C H. Multifunctional bionanocomposite films based on konjac glucomannan/chitosan with nano-ZnO and mulberry anthocyanin extract for active food packaging. *Food Hydrocolloids*, 2020, 107: 105942
14. Kan J, Liu J, Xu F, Yun D W, Yong H M, Liu J. Development of pork and shrimp freshness monitoring labels based on starch/polyvinyl alcohol matrices and anthocyanins from 14 plants: a comparative study. *Food Hydrocolloids*, 2022, 124: 107293
15. Vidana Gamage G C, Lim Y Y, Choo W S. Black goji berry anthocyanins: extraction, stability, health benefits, and applications. *ACS Food Science and Technology*, 2021, 1(8): 1360–1370
16. Qin Y, Yun D W, Xu F F, Chen D, Kan J, Liu J. Smart packaging films based on starch/polyvinyl alcohol and *Lycium ruthenicum* anthocyanins-loaded nano-complexes: functionality, stability and application. *Food Hydrocolloids*, 2021, 119: 106850
17. Qin Y, Liu Y P, Yong H M, Liu J, Zhang X, Liu J. Preparation and characterization of active and intelligent packaging films based on cassava starch and anthocyanins from *Lycium ruthenicum* Murr. *International Journal of Biological Macromolecules*, 2019, 134: 80–90
18. Liu D F, Cui Z J, Shang M, Zhong Y F. A colorimetric film based on polyvinyl alcohol/sodium carboxymethyl cellulose incorporated with red cabbage anthocyanin for monitoring pork freshness. *Food Packaging and Shelf Life*, 2021, 28: 100641
19. Lan W J, Wang S Y, Zhang Z J, Liang X, Liu X W, Zhang J. Development of red apple pomace extract/chitosan-based films reinforced by TiO₂ nanoparticles as a multifunctional packaging material. *International Journal of Biological Macromolecules*, 2021, 168: 105–115
20. Rawdkuen S, Faseha A, Benjakul S, Kaewprachu P. Application of anthocyanin as a color indicator in gelatin films. *Food Bioscience*, 2020, 36: 100603
21. Li Y N, Ye Q Q, Hou W F, Zhang G Q. Development of antibacterial ϵ -polylysine/chitosan hybrid films and the effect on citrus. *International Journal of Biological Macromolecules*, 2018, 118: 2051–2056
22. Ren J Z, Li Y N, Lin Q B, Li Z H, Zhang G Q. Development of biomaterials based on plasticized polylactic acid and tea polyphenols for active-packaging application. *International Journal of Biological Macromolecules*, 2022, 217: 814–823
23. Qin Y, Yun D W, Xu F F, Li C C, Chen D, Liu J. Impact of storage conditions on the structure and functionality of starch/polyvinyl alcohol films containing *Lycium ruthenicum* anthocyanins. *Food Packaging and Shelf Life*, 2021, 29: 100693
24. Wang Y W, Li Y N, Lin Q B, Wang X, Li Z H, Wu K X. Functional and antioxidant properties of plastic bottle caps incorporated with BHA or BHT. *Materials*, 2021, 14(16): 1–15
25. Alizadeh-Sani M, Tavassoli M, Mohammadian E, Ehsani A, Khaniki G J, Priyadarshi R, Rhim J W. pH-responsive color indicator films based on methylcellulose/chitosan nanofiber and barberry anthocyanins for real-time monitoring of meat freshness. *International Journal of Biological Macromolecules*, 2021, 166: 741–750
26. Kumar N, Pratibha, Trajkovska Petkoska A, Khojah E, Sami R, Al-Mushhin A A M. Chitosan edible films enhanced with pomegranate peel extract: study on physical, biological, thermal, and barrier properties. *Materials*, 2021, 14(12): 3305
27. Yong H M, Wang X C, Bai R Y, Miao Z Q, Zhang X, Liu J. Development of antioxidant and intelligent pH-sensing packaging films by incorporating purple-fleshed sweet potato extract into chitosan matrix. *Food Hydrocolloids*, 2019, 90: 216–224
28. Qin Y, Liu Y P, Zhang X, Liu J. Development of active and intelligent packaging by incorporating betalains from red pitaya (*Hylocereus polyrhizus*) peel into starch/polyvinyl alcohol films. *Food Hydrocolloids*, 2020, 100: 105410
29. Oliveira Filho J G, Braga A R C, Oliveira B R, Gomes F P, Moreira V L, Pereira V A C, Egea M B. The potential of anthocyanins in smart, active, and bioactive eco-friendly polymer-based films: a review. *Food Research International*, 2021, 142: 110202
30. Priyadarshi R, Negi Y S. Effect of varying filler concentration on zinc oxide nanoparticle embedded chitosan films as potential food packaging material. *Journal of Polymers and the Environment*, 2017, 25(4): 1087–1098
31. Yan J T, Zhang H, Yuan M L, Qin Y Y, Chen H Y. Effects of anthocyanin-rich *Kadsura coccinea* extract on the physical, antioxidant, and pH-sensitive properties of biodegradable film. *Food Biophysics*, 2022, 17(3): 375–385
32. Rahman P M, Mujeeb V M A, Muraleedharan K. Flexible chitosan-nano ZnO antimicrobial pouches as a new material for extending the shelf life of raw meat. *International Journal of Biological Macromolecules*, 2017, 97: 382–391
33. Merz B, Capello C, Leandro G C, Moritz D E, Monteiro A R, Valencia G A. A novel colorimetric indicator film based on chitosan, polyvinyl alcohol and anthocyanins from jambolan (*Syzygium cumini*) fruit for monitoring shrimp freshness. *International Journal of Biological Macromolecules*, 2020, 153: 625–632
34. Halász K, Csóka L. Black chokeberry (*Aronia melanocarpa*) pomace extract immobilized in chitosan for colorimetric pH indicator film application. *Food Packaging and Shelf Life*, 2018, 16: 185–193
35. Singh S, Nwabor O F, Syukri D M, Voravuthikunchai S P. Chitosan-poly(vinyl alcohol) intelligent films fortified with anthocyanins isolated from *Clitoria ternatea* and *Carissa carandas* for monitoring beverage freshness. *International Journal of Biological Macromolecules*, 2021, 182: 1015–1025
36. Li Y, Zhou Y, Wang Z L, Cai R, Yue T L, Cui L. Preparation and characterization of chitosan-nano-ZnO composite films for preservation of cherry tomatoes. *Foods*, 2021, 10(12): 3135

37. Mujeeb Rahman P, Abdul Mujeeb V M, Muraleedharan K, Thomas S K. Chitosan/nano ZnO composite films: enhanced mechanical, antimicrobial and dielectric properties. *Arabian Journal of Chemistry*, 2018, 11(1): 120–127
38. Hou J M, Yan X X. Preparation of chitosan-SiO₂ nanoparticles by ultrasonic treatment and its effect on the properties of starch film. *International Journal of Biological Macromolecules*, 2021, 189: 271–278
39. Khan S A, Rahman A, Ibrahim F B D A. The impact of film thickness on the properties of ZnO/PVA nanocomposite film. *Materials Research Express*, 2021, 8(7): 075002
40. Roy S, Rhim J W. Carboxymethyl cellulose-based antioxidant and antimicrobial active packaging film incorporated with curcumin and zinc oxide. *International Journal of Biological Macromolecules*, 2020, 148: 666–676
41. Ezati P, Rhim J W. pH-responsive chitosan-based film incorporated with alizarin for intelligent packaging applications. *Food Hydrocolloids*, 2020, 102: 105629
42. Shen R Y, Wang H J, Wu K Z, Gao J, Li J B. Characterization and antimicrobial properties of ferulic acid grafted self-assembled bacterial cellulose-chitosan membranes. *Journal of Applied Polymer Science*, 2021, 138(33): 1–13
43. Sun X H, Zhou T T, Wei C H, Lan W Q, Zhao Y, Pan Y J, Wu V C H. Antibacterial effect and mechanism of anthocyanin rich Chinese wild blueberry extract on various foodborne pathogens. *Food Control*, 2018, 94: 155–161
44. Dong H L, Ling Z, Zhang X, Zhang X M, Ramaswamy S, Xu F. Smart colorimetric sensing films with high mechanical strength and hydrophobic properties for visual monitoring of shrimp and pork freshness. *Sensors and Actuators B: Chemical*, 2020, 309: 127752